

Predicted quantum stripe ordering in optical lattices

Congjun Wu,¹ W. Vincent Liu,² Joel Moore,^{3,4} and Sankar Das Sarma⁵

¹Kavli Institute for Theoretical Physics, University of California, Santa Barbara, CA 93106

²Department of Physics and Astronomy, University of Pittsburgh, Pittsburgh, PA 15260

³Department of Physics, University of California, Berkeley, CA 94720

⁴Materials Sciences Division, Lawrence Berkeley National Laboratory, Berkeley CA 94720

⁵Condensed Matter Theory Center, Department of Physics,
University of Maryland, College Park, MD 20742

We predict the robust existence of a novel quantum orbital stripe order in the p-band Bose-Hubbard model of two-dimensional triangular optical lattices with cold bosonic atoms. An orbital angular momentum moment is formed on each site exhibiting a stripe order both in the superfluid and Mott-insulating phases. The stripe order spontaneously breaks time-reversal, lattice translation and rotation symmetries. In addition, it induces staggered plaquette bond currents in the superfluid phase. Possible signatures of this stripe order in the time-of-flight experiment are discussed.

PACS numbers: 03.75.Lm, 05.30.Jp, 73.43.Nq, 74.50.+r

Cold atomic systems with multiple internal components, such as large spin systems, exhibit much richer phase diagrams and properties than the usual spinless bosons and spin- $\frac{1}{2}$ fermions. For example, various spinor condensations and spin dynamics have been investigated in spin-1 systems [1, 2]. Similarly, large spin fermions also exhibit many novel features, including hidden symmetries [3], quintet Cooper pairing states and associated topological defects [4], and multiple-particle clustering instabilities [5]. Motivated by such considerations, but for orbital degeneracy, we investigate the p-band Bose-Hubbard (BH) model for cold atom optical lattices, finding a novel quantum orbital stripe phase in triangular bosonic p-band optical lattices.

In solid state physics, orbital dynamics plays important roles in transition metal oxides leading to interesting phenomena, such as orbital ordering and colossal magnetoresistance [6]. In optical lattices, pioneering experiments on orbital physics have been recently carried out by Browaeys et. al [7] by accelerating the lattice of bosons, and by Kohl et. al [8] by using fermionic Feshbach resonance. These experiments demonstrate the population of higher orbital bands, motivating our theoretical interest in possible orbital ordering in cold atom optical lattices. In particular, the p-band bosons in the square or cubic lattices, which exhibit qualitatively new features compared to their s-wave counterpart, have received much attention [9, 10, 11, 12]. For example, Ref. [10] focuses on the sub-extensive Z_2 symmetry [13, 14, 15] and the resulting nematic superfluid order by considering only the σ -type bonding in the band structure. By further keeping the π -bonding term, the ground state is shown to break time reversal (TR) symmetry spontaneously, forming an antiferromagnetic order of orbital angular momentum (OAM) moments [11, 12]. Various methods to excite bosons to the p-band and maintain bosons there for a long time have been suggested in Ref. [9, 10, 11, 12].

The p-band bosons in a frustrated optical lattice have, however, not been fully studied yet. In this paper, we study the quantum phases of the p-band BH model in a 2D triangular lattice, finding a novel quantum stripe ordering. The onsite Hubbard interaction gives rise to a Hund's rule-like coupling in the OAM channel, resulting in the formation of an Ising OAM moment on each site. Due to the geometric frustration inherent in the triangular lattice, the ground state exhibits a stripe order of the OAM moments which spontaneously breaks TR, lattice rotation and translation symmetries. In the superfluid (SF) phase, the stripe order further induces the staggered plaquette bond currents, reminiscent of the d-density wave proposal for the pseudogap phase in high T_c cuprates [16]. This stripe order bears some special similarity to its solid-state counterpart observed in strongly correlated electronic systems, such as manganites [17], high T_c cuprates [18], and high-Landau level quantum Hall systems [19], but is different qualitatively since, unlike the solid-state examples, the stripe order in the p-band bosonic triangular optical lattices is fully quantum in nature and does not just arise from the long-range Coulomb interaction. We show that the stripe order persists deep in the Mott-insulating (MI) phase even with the disappearance of superfluidity.

We begin with the construction of the p-band BH model in a 2D (x-y) triangular lattice. The optical potential on each site is approximated by a 3D anisotropic harmonic potential with frequencies $\omega_z \neq \omega_x = \omega_y$. Thus we can neglect the p_z -band, and only consider a two-band model of p_x and p_y . We define three unit vectors $\hat{e}_1 = \hat{e}_x; \hat{e}_{2;3} = \frac{1}{2}\hat{e}_x - \frac{\sqrt{3}}{2}\hat{e}_y$, and the two primitive lattice vectors can be taken as $a_0\hat{e}_{1;2}$ (a_0 the lattice constant). The projection of the $p_{x;y}$ orbitals along the $\hat{e}_{1;2;3}$ directions are $p_1 = p_x; p_{2;3} = \frac{1}{2}p_x - \frac{\sqrt{3}}{2}p_y$. Due to the anisotropic nature of the p-orbitals, the hopping terms are dominated by the "head to tail" type σ -bonding (the

-bonding t_z term can be neglected here) as

$$H_0 = t_k \sum_{\mathbf{x}; i=1,2,3} \sum_n p_{i,\mathbf{x}}^y p_{i,\mathbf{x}+\mathbf{e}_i} + h.c.; \quad (1)$$

where t_k is positive due to the odd parity of the p-orbitals. The on-site Hubbard repulsion H_{int} can be calculated from the contact interaction of coupling constant g :

$$H_{int} = \frac{U}{2} \sum_{\mathbf{x}} \sum_n n_{\mathbf{x}}^2 - \frac{1}{3} L_{z,\mathbf{x}}^2; \quad (2)$$

with $n_{\mathbf{x}}$ the particle number and $L_z = i(\hat{p}_y \hat{p}_x - \hat{p}_x \hat{p}_y)$ the z-component OAM; $U = 3g = [4(2)^{3=2} \frac{1}{k_x k_y k_z}]$ with $k_i = \frac{h}{m v_i}$ ($i = x, y, z$). The important feature of H_{int} is its ferro-orbital nature [1] which is analogous to the Hund's rule for atomic electrons. This implies that bosons on each site prefer to go into the axial states of p_x or p_y . This is because the axial states are spatially more extended than the polar states p_x, p_y , and thus are energetically more favorable for $g > 0$.

We first consider the weak coupling limit, $U \rightarrow 0$. The Brillouin zone takes the shape of a regular hexagon with the edge length $a = 3a_0$. The energy spectrum of H_0 is $E(\mathbf{k}) = t_k f_{\mathbf{k}} - \frac{f_{\mathbf{k}}^2}{3g_{\mathbf{k}}}$; where $f_{\mathbf{k}} = \sum_{i=1}^3 \cos(\mathbf{k} \cdot \mathbf{e}_i)$ and $g_{\mathbf{k}} = \sum_{i>j=1}^3 \cos(\mathbf{k} \cdot \mathbf{e}_i) \cos(\mathbf{k} \cdot \mathbf{e}_j)$. The spectrum contains three degenerate minima located at $K_1 = (0; \frac{2}{3a}; \frac{2}{3a})$; $K_2 = (\frac{a}{3}; \frac{2}{3a}; \frac{2}{3a})$, and $K_3 = (\frac{a}{3}; \frac{2}{3a}; \frac{2}{3a})$. The factor $e^{i\mathbf{k} \cdot \mathbf{e}_i}$ takes the value of ± 1 uniformly in each horizontal row but alternating in adjacent rows. If the above pattern is rotated at angles of $\frac{2}{3}$, then we arrive at the patterns of $e^{i\mathbf{k} \cdot \mathbf{e}_i}$. Each eigenvector is a 2-component superposition vector of p_x and p_y orbitals. The eigenvectors at energy minima are $\mathbf{K}_1 = e^{i\mathbf{k} \cdot \mathbf{e}_1} \begin{pmatrix} 1 \\ j_1 \end{pmatrix}$ with $j_1 = \frac{1}{2} \frac{p_y}{p_x}$; $\mathbf{K}_{2,3} = e^{i\mathbf{k} \cdot \mathbf{e}_2} \begin{pmatrix} j_2 \\ 1 \end{pmatrix}$ with $j_{2,3} = \frac{1}{2} \frac{p_x}{p_y}$. $\mathbf{K}_{2,3}$ can be obtained by rotating \mathbf{K}_1 at angles of $\frac{2}{3}$ respectively.

The ground state condensate wavefunction ψ_c can be constructed as follows. Any linear superposition of the three band minima $\psi_c(\mathbf{x}) = c_1 \mathbf{K}_1 + c_2 \mathbf{K}_2 + c_3 \mathbf{K}_3$ with the constraint $|c_1|^2 + |c_2|^2 + |c_3|^2 = 1$ equally minimizes the kinetic energy H_0 . However, an infinitesimal $U \rightarrow 0$ removes the band degeneracy to further optimize the interaction energy H_{int} . After straightforward algebra, we find the optimal configurations occur at $c_1 = 0; c_2 = \frac{1}{2}; c_3 = \frac{1}{2}$, and its symmetrically equivalent partners. Thus the mean field condensate can be expressed as $\frac{1}{2} (\frac{y}{K_2} + i \frac{y}{K_3}) \sum_{\mathbf{j}} \psi_{\mathbf{j}}$ with $\psi_{\mathbf{j}}$ the vacuum state and N_0 the particle number in the condensate. This state breaks the $U(1)$ gauge symmetry, as well as TR and lattice rotation symmetries, thus the ground state manifold is $U(1) \times Z_2 \times Z_3$. This state also breaks lattice translation symmetry, which is, however, equivalent to

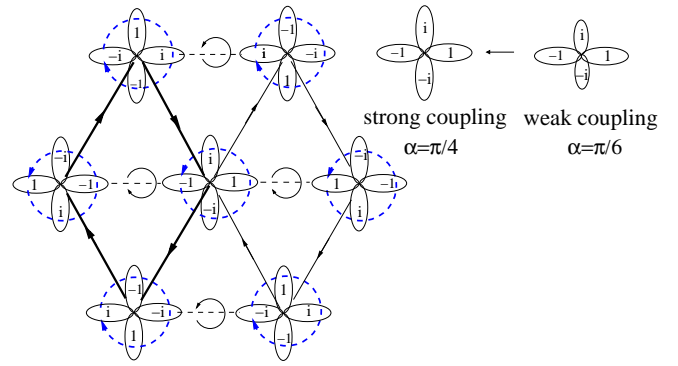


FIG. 1: The condensate configuration in the real space described by Eq.(3) with TR, rotation, and $U(1)$ symmetry breaking. The unit cell contains 4 sites as marked with thick lines. The OAM moments (dashed arrowed circles) form the stripe order, and induce bond currents exhibiting staggered plaquette moments (solid arrowed circles). In Eq. 3 depends on the interaction strength with $\alpha = \frac{\pi}{6}$ ($\frac{\pi}{4}$) in the strong (weak) coupling limit respectively. Currents vanish in the weak coupling limit, and exist on tilted bonds at finite interaction strength with directions specified by arrows.

suitable combinations of $U(1)$ and lattice rotation operations.

For better insight, we transform the above momentum space condensate to the real space. The orbital configuration on each site reads

$$e^{i\mathbf{x} \cdot \mathbf{K}_1} (\cos \mathbf{p}_x \mathbf{i} + i \sin \mathbf{p}_y \mathbf{j}) \quad (3)$$

with $\mathbf{K}_1 = \frac{2}{3}$ as $U \rightarrow 0$. The general configuration of ψ_c is depicted in Fig. 1 for later convenience. The $U(1)$ phase \mathbf{p}_x is specified at the right lobe of the p-orbital. The Ising variable $\sigma_{\mathbf{x}} = \pm 1$ denotes the direction of the OAM, and is represented by the anti-clockwise (clockwise) arrow on each site. As expected from the Hund's rule interaction, each site exhibits a nonzero OAM and breaks TR symmetry. At $U \rightarrow 0$, p_x, p_y are not equally populated, and the moment per particle is $\frac{1}{2} \frac{h}{m}$. This does not fully optimize H_{int} which requires $L_{z,\mathbf{x}} = \frac{1}{2} h$. However, it indeed fully optimizes H_0 which dominates over H_{int} in the weak coupling limit. We check that the phase difference is zero along each bond, and thus no inter-site bond current exists. Interestingly, as depicted in Fig. 1, OAM moments form a stripe order along each horizontal row. The driving force for this stripe formation in the SF regime is the kinetic energy, i.e., the phase coherence between bosons in each site. By contrast, the stripe formation in high T_c cuprates (or other solid-state systems, e.g. manganites and quantum Hall systems) is driven by the competition between long range repulsion and the short range attraction in the interaction terms [18].

Next we discuss the ordering in the strong coupling SF regime. For large values of $U \rightarrow 0$, we first minimize H_{int} with n particles per site. For simplicity, we consider the

large n case, then Hund's rule coupling favors the onsite state $(\cos \frac{\pi}{4} p_x^y + i \sin \frac{\pi}{4} p_y^y) |j\rangle$. This corresponds to the case $\theta = \frac{\pi}{4}$ in Fig. 1 where $p_{x,y}$ orbitals are equally populated. Because of the anisotropic orientation of the p -orbitals, the phase difference between two sites along each bond not only depends on the $U(1)$ and the Ising variables, but also on the direction of the bond as in the $p + ip$ Josephson junction arrays [13]. This effect can be captured by a $U(1)$ gauge field. The effective Hamiltonian then reads $H_{\text{eff}} = \frac{1}{2} \sum_{\mathbf{k}} n_{\mathbf{k}} \cos \theta_{\mathbf{r}_1; \mathbf{r}_2} + \frac{1}{3} U \sum_{\mathbf{r}_1; \mathbf{r}_2} n_{\mathbf{r}_1}^2$; where the gauge field $\theta_{\mathbf{r}_1; \mathbf{r}_2} = \theta_{\mathbf{r}_1; \mathbf{r}_2} + \theta_{\mathbf{r}_2; \mathbf{r}_1}$ is the angle between the bond from \mathbf{r}_1 to \mathbf{r}_2 and the x -axis, and thus $\theta_{\mathbf{r}_2; \mathbf{r}_1} = \theta_{\mathbf{r}_1; \mathbf{r}_2} + \pi$. The external gauge flux in the plaquette i with three vertices $\mathbf{r}_{1,2,3}$ can be calculated as

$$\theta_i = \frac{1}{2} \sum_{\mathbf{r}; \mathbf{r}' \in i} \theta_{\mathbf{r}; \mathbf{r}'} = \frac{1}{6} (\theta_{\mathbf{r}_1; \mathbf{r}_2} + \theta_{\mathbf{r}_2; \mathbf{r}_3} + \theta_{\mathbf{r}_3; \mathbf{r}_1}) \text{ mod } 1. \quad (4)$$

Following the analysis in Ref. [13, 20], the ground state configuration for Ising variables requires the flux θ_i (vorticity) in each plaquette to be as small as possible, which are just $\frac{1}{6}$ corresponding to Ising variables of two ± 1 's and one -1 .

The stripe order persists in the strong coupling SF regime due to the interaction among vortices. The dual lattice is the bipartite honeycomb lattice, thus it is tempting to assign $\frac{1}{6}$ alternatively to each plaquette. However, this is not possible. Consider a plaquette with vorticity $+\frac{1}{6}$, thus its three vertices are with two $+1$'s and one -1 . The neighbouring plaquette sharing the edge with two $+1$'s must have the same vorticity, and merges with the former one to form a rhombic plaquette with the total vorticity $+\frac{1}{3}$. Thus the ground state should exhibit a staggered pattern of rhombic plaquettes with vorticity of $\frac{1}{3}$. The stripe pattern of OAM moments is the only possibility to satisfy this requirement. The stripe phase obtained here is quite general: for example, it will also appear in the triangular-lattice $p + ip$ Josephson-junction array [13] if tunneling is dominated by the momentum-reversing process [20], rather than by the momentum-conserving process that gives a uniform state. This stripe ordering possibility in the triangular $p + ip$ Josephson junction arrays has not been earlier appreciated.

In addition, the stripe order results in the staggered bond currents as depicted in Fig. 1. We further optimize the $U(1)$ phase variables, and find that their pattern is the same as that in the weak coupling limit. Taking into account the equal weight of $p_{x,y}$ in each site, we find no phase mismatch along each horizontal bond, but a phase mismatch of $\theta = \frac{\pi}{6}$ along each tilted bond. As a result, on each bond around the rhombic plaquette, the Josephson current is $j = \frac{tn_0}{2} \sin \theta$ where $n_0 = n$ is the condensate fraction, and the current direction is specified by arrows in Fig. 1. The total phase winding around each

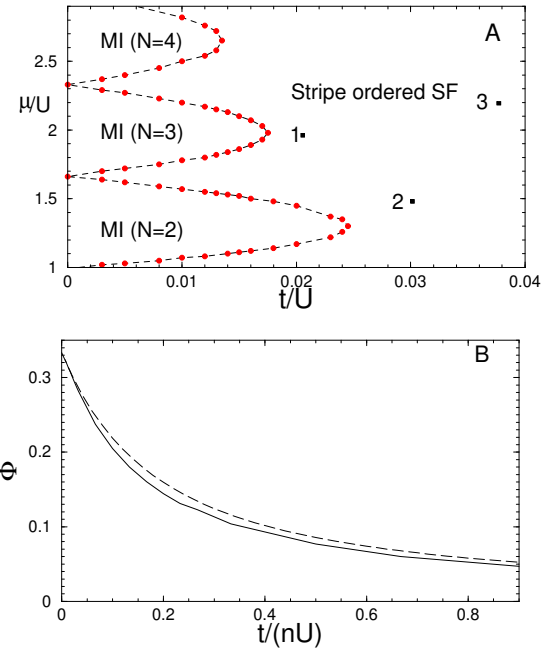


FIG. 2: A) Phase diagram based on the GMF theory in the 2×2 unit cell (see Fig. 1). Large scale GMF calculations in a 30×30 lattice are performed to confirm the stripe ordered superfluid (SF) phase at points 1, 2 and 3 with $(t/U; U/U) = (0.02; 2); (0.03; 1.5)$ and $(0.038; 2.2)$, respectively. B) The flux around a rhombic plaquette v.s. $t/(nU)$. It decays from $\frac{1}{3}$ in the strong coupling limit to 0 in the non-interaction limit. The solid line is the GMF result at $n = 3$, while the dashed line is based on the energy function Eq. 5 of the trial condensate.

rhombic plaquette is $4 \times \frac{\pi}{6} = \frac{2\pi}{3}$, and thus agrees with the vorticity of $\frac{1}{3}$. This staggered plaquette bond current is similar to the d -density wave state proposed in high- T_c cuprates [16], but with a completely different microscopic origin. We emphasize that the p -band square lattice case does not have this interesting physics [11].

Since the stripe order exists in both strong and weak coupling limits, it should also exist at intermediate coupling strength. We have confirmed this conjecture using the Gutzwiller mean field (GMF) theory in a 30×30 lattice for three systems (marked as points 1, 2, and 3 in Fig. 2). We find that the stripe ordered ground state is stable against small perturbations in all three cases. We further apply the GMF theory to the 2×2 unit cell (Fig. 1), and obtain the phase diagram of the stripe ordered SF and MI phases (Fig. 2A). For the GMF numerical results, we write the trial condensate with the p -orbital occupation on each site as $e^{i\theta} (\cos \theta p_x + i \sin \theta p_y)$. The angle $\frac{\theta}{2} > 0$ describes the relative weight of p_x and p_y orbitals. It turns out that the pattern for the $U(1)$ phase does not depend on θ , and remains the same for all the coupling strength. The phase mismatch on the tilted

- [2] T. L. Ho, et al, Phys. Rev. Lett. 81, 742 (1998); T. Ohm i et al., J. Phys. Soc. Jpn., 67, 1822 (1998); E. Demler et al, Phys. Rev. Lett. 88, 163001 (2002); F. Zhou, Phys. Rev. Lett. 87, 80401 (2001).
- [3] C. Wu et al, Phys. Rev. Lett. 91, 186402 (2003).
- [4] C. Wu et al, cond-m at/0512602; T. L. Ho et al, Phys. Rev. Lett. 82, 247 (1999).
- [5] C. Wu, Phys. Rev. Lett. 95, 266404 (2005); P. Lecheminant et al, Phys. Rev. Lett. 95, 240402 (2005).
- [6] Y. Tokura and N. Nagaosa, Science 288, 462 (2000).
- [7] A. Browaeys et. al, Phys. Rev. A 72 53605 (2005).
- [8] M. Kohler et. al, Phys. Rev. Lett. 94, 80403 (2006).
- [9] V. W. Scarola et. al, Phys. Rev. Lett. 65, 33003 (2005).
- [10] A. Isacsson et. al, Phys. Rev. A 72, 053604 (2005).
- [11] W. V. Liu and C. Wu, cond-m at/0601432.
- [12] A. B. Kuklov, cond-m at/0601416.
- [13] J. E. Moore et al, Phys. Rev. B 69, 104511 (2004).
- [14] C. Xu et al, Phys. Rev. Lett. 93, 47003 (2004).
- [15] Z. Nussinov, et. al, Phys. Rev. B 71, 195120 (2005).
- [16] S. Chakravarty et al, Phys. Rev. B 63, 94503 (2001).
- [17] S. Mori et al, Nature 392, 473 (1998).
- [18] S. A. Kivelson, et. al, Rev. Mod. Phys. 75, 1201 (2003).
- [19] M. P. Lilly et al, Phys. Rev. Lett. 82, 394 (1999); R. Du et al, Solid State Commun. 109, 389 (1999).
- [20] C. Castelnovo et al, Phys. Rev. B 69, 104529 (2004).
- [21] J. Stephenson, J. Math. Phys. 5, 1009 (1964).